Research Square

Preprints are preliminary reports that have not undergone peer review.
They should not be considered conclusive, used to inform clinical practice,
or referenced by the media as validated information.

Load-Associated Sacroiliac Joint Space Narrowing Is Associated with Positional Pelvic Incidence Discordance: A Three-Dimensional Weight-Bearing CT Study

Subin Lim
Korea University Guro Hospital
Hong Jin Kim
Korea University Guro Hospital
Seung Woo Suh
Korea University Guro Hospital
Suk-Ha Lee
Konkuk University Medical Center
Tae-Hoon Kim
Konkuk University Medical Center
Min-Seok Kang
Konkuk University Medical Center
HyungRae Lee
Korea University Anam Hospital
Dong-Gune Chang
Inje University Sanggye Paik Hospital
Jae Hyuk Yang
gurospine@naver.com

Korea University Anam Hospital

Research Article

Keywords: pelvic incidence, weight-bearing CT, sacroiliac joint, micromotion, spinopelvic alignment

Posted Date: November 19th, 2026

DOI: https://doi.org/10.21203/rs.3.rs-10583642/v1

License: This work is licensed under a Creative Commons Attribution 4.0 International License.
Read Full License

Additional Declarations: No competing interests reported.

Abstract

Background

Pelvic incidence (PI) has traditionally been considered a fixed anatomical parameter. However, recent weight-bearing CT (WBCT) studies suggest that PI may vary functionally under physiological loading. The biomechanical mechanisms underlying this phenomenon remain unclear. This study investigated whether dynamic sacroiliac (SI) joint micromotion contributes to functional PI alteration using a three-dimensional WBCT-based analysis framework.

Methods

Fifty older adult patients with degenerative lumbar disorders who underwent both WBCT and non–weight-bearing CT (NWBCT) were prospectively enrolled. A three-dimensional CT-based framework was used to calculate spinopelvic parameters, including PI, pelvic tilt (PT), sacral slope (SS), and left–right PI asymmetry. Quantitative SI joint parameters, including SI joint space width (JSW), SI angle, and S1 subsidence, were additionally evaluated. Correlation and regression analyses were performed to identify biomechanical factors associated with PI change (ΔPI).

Results

PI increased on WBCT versus NWBCT (52.04 ± 10.14° vs. 49.35 ± 9.90°; mean Δ = 2.69°; 95% CI, 1.62°–3.75°; Cohen's d_z = 0.72; $p < 0.001$). The PI interobserver agreement was excellent (ICC (2,1) = 0.954). The mean ΔPI exceeded the cohort-level MDC_{95}(1.02°). Under loading, PT and S1 subsidence increased, while SS, SI angle, and bilateral SI joint space widths (JSW) decreased (all $p < 0.001$). Greater bilateral JSW narrowing correlated with larger ΔPI (right: $r = -0.433$, $p = 0.0017$; left: $r = -0.335$, $p = 0.0173$). ΔSS and ΔS1-femur coronal angle independently contributed to loading-related PI variability ($R^2 = 0.274$, $p < 0.0001$).

Conclusions

Functional PI alteration under physiological loading is strongly associated with 3D morphological deformation of the SI joint. The significant correlation between bilateral SI joint space narrowing and ΔPI suggests that load-dependent PI variability reflects actual articular compression and micromotion rather than positional artifacts. These findings highlight the importance of considering dynamic SI joint behavior in spinopelvic assessment.

Introduction

Assessment of spinopelvic alignment is essential for understanding the pathophysiology and compensatory mechanisms of degenerative spinal disorders.(1–3) Traditionally, parameters such as pelvic incidence (PI), pelvic tilt (PT), and sacral slope (SS) have been evaluated using standing two-dimensional (2D) whole-spine radiographs.(4, 5) Among these parameters, PI has long been regarded as a constant morphological descriptor unique to each individual.(6, 7) However, 2D imaging is inherently limited by anatomical superimposition and variations in patient posture.(1, 8) Although three-dimensional (3D) imaging modalities, such as computed tomography (CT) provide superior anatomical resolution, conventional non–weight-bearing CT (NWBCT), acquired in the supine position, does not adequately reflect the biomechanical environment of the spine and pelvis under physiological loading conditions.(9)

Recent investigations using weight-bearing CT (WBCT) have demonstrated that spinopelvic alignment changes dynamically under gravitational loading and that PI may vary functionally with posture rather than behave as a rigid anatomical constant.(10–13) Despite these findings, the biomechanical basis underlying PI variation remains incompletely understood. We hypothesized that postural changes in PI are not merely attributable to projectional or measurement-related artifacts but instead reflect 3D deformation of the sacroiliac (SI) joint under physiological loading conditions.

Therefore, this study aimed to investigate the 3D biomechanical mechanisms underlying functional PI variation. Using a WBCT-based 3D analysis framework, we quantitatively evaluated novel SI joint parameters, including joint space width (JSW), sacral subsidence, and SI angle, alongside conventional spinopelvic parameters. Dynamic changes between non–weight-bearing and weight-bearing conditions were subsequently analyzed.

Methods

Study Design and Participants

This study was a secondary biomechanical analysis of prospectively acquired data from a single-center observational cohort. The study was approved by the Institutional Review Board of Korea University Anam Hospital (IRB No. 2024AN0427) and was conducted in accordance with the ethical principles of the Declaration of Helsinki and the Strengthening the Reporting of Observational Studies in Epidemiology (STROBE) guidelines. Written informed consent to participate was obtained from all participants prior to enrollment. Patients presenting to the outpatient spine clinic between December 2024 and March 2025 were consecutively enrolled. The inclusion criteria were: (1) age ≥ 19 years; (2) a diagnosis of a degenerative or deformative lumbar spinal disorder established by a spine specialist; and (3) availability of paired standing weight-bearing CT (WBCT) and supine non–weight-bearing CT (NWBCT), together with the required radiographic examinations. The exclusion criteria were: (1) inability to ambulate independently because of severe cardiopulmonary, hepatic, or renal dysfunction; (2) a neuromuscular disorder affecting lower-extremity strength or weight-bearing capacity; and (3) inability to maintain a

stable standing posture during WBCT acquisition. A total of 50 patients met the eligibility criteria and were included in the analysis.

The demographic characteristics, imaging acquisition protocol, basic three-dimensional spinopelvic measurement framework, and positional discordance in conventional spinopelvic parameters within this cohort have been reported previously(13). The present study addressed a distinct biomechanical hypothesis by applying a previously unreported sacroiliac joint–specific quantitative analysis protocol to the paired imaging dataset. This protocol included measurements of bilateral sacroiliac joint space width, SI joint angle, and relative S1 position, together with dedicated reliability and measurement-error analyses, to determine whether load-associated differences in SI joint geometry were associated with positional pelvic incidence discordance. None of these SI joint–specific measurements or analyses was included in the previous publication.

Radiographic Evaluation of Spinopelvic Parameters

Spinopelvic parameters were measured on standing and supine lateral radiographs using an institutional picture archiving and communication system (PACS). PI was defined as the angle between the line perpendicular to the midpoint of the superior S1 endplate and the line connecting this point to the bicoxofemoral axis. PT was defined as the angle between the vertical reference line and the line connecting the midpoint of the sacral endplate to the bicoxofemoral axis. The sacral slope (SS) was defined as the angle between the superior S1 endplate and horizontal plane.(6, 14) To evaluate coronal pelvic orientation, the S1-to-femur coronal angle (S1FCA) was measured on anteroposterior radiographs. S1FCA was defined as the angle between the superior S1 endplate line and the line connecting the centers of both femoral heads **(**Fig. 1-a**).**

Sacroiliac Joint (SI) Vacuum Phenomenon

Vacuum phenomena within the SI joint were assessed using axial, sagittal, and coronal CT tomography. The sacroiliac (SI) joint was subdivided into ventral cartilaginous and dorsal ligamentous regions.(15) The presence or disappearance of vacuum clefts between the NWBCT and WBCT was recorded separately for both SI joints and interpreted as a potential indicator of dynamic SI joint micromotion or instability under loading conditions **(**Fig. 1-b **and c).**

3D CT-Based Spinopelvic Measurement Framework

In the present study, a previously developed WBCT-based 3D analysis framework was used for spinopelvic assessment.(13) The framework was implemented using a Python-based Visualization Toolkit (VTK) environment and enabled geometric reconstruction of pelvic anatomical landmarks from DICOM image datasets.

For WBCT, patients were instructed to stand upright. NWBCT was performed in the supine position. Following CT acquisition, anatomical landmark coordinates identified on coronal, sagittal, and axial multiplanar reconstruction views were transformed from pixel space into physical three-dimensional coordinates (millimeters) using DICOM spacing information.

The centers of both femoral heads were manually identified and reconstructed in 3D space. The midpoint between the femoral head centers was defined as the pelvic center (Pmid). The anterior and posterior endpoints of the superior sacral endplate were selected on sagittal images, and the midpoint of the endplate was defined as the sacral center point (Ps). The normal vector perpendicular to the superior sacral endplate was defined as the sacral vector (Vs).

Using these reference coordinates, PI was calculated as the angle between the vector connecting Pmid and Ps and the Vs. PT was calculated as the angle between the vertical axis and line connecting Pmid and Ps, while SS was defined as the angle between Vs and horizontal ground plane. This framework additionally enabled separate calculations of the left and right pelvic incidences using each femoral head center independently. The absolute difference between left and right PI values was defined as ΔPI asymmetry **(**Fig. 2**).**

Quantitative Evaluation of SI Joint Micromotion

To evaluate the dynamic SI joint deformation under loading conditions, multiplanar reconstruction planes parallel to the S1 foramina were generated in both the WBCT and NWBCT datasets. Measurements were performed at the corresponding anatomical levels under both imaging conditions.

SI Joint Space Width (JSW) and SI Joint Angle (SI angle)

The sacroiliac joint space width (JSW) was defined for the purposes of this study, as the minimum distance between the sacral and iliac articular surfaces at the S1 foramina-parallel plane level. The right and left SI joints were evaluated separately. Changes in JSW between the WBCT and NWBCT were calculated to quantify the compressive narrowing of the SI joint under weight-bearing conditions. The SI angle was measured on the S1 foramina-parallel plane as the angle between the bilateral iliac cortical lines. A decreased SI angle under weight-bearing conditions was interpreted as the converging motion of the iliac wings associated with SI joint compression **(**Fig. 3**).**

S1 Subsidence

To evaluate the inferior displacement of the sacrum during weight bearing, S1 subsidence was defined as the perpendicular distance between the iliac crest reference line and anterior tip of the S1 vertebral body on the reconstructed S1 endplate-parallel plane. Increased WBCT values were interpreted as an inferior migration of the sacrum relative to the iliac ring **(**Fig. 4**).**

Statistical Analysis

All statistical analyses were performed using IBM SPSS Statistics version 29 (IBM Corp., Armonk, NY, USA). Continuous variables were expressed as the mean ± standard deviation. Normality was evaluated using the Shapiro–Wilk test.

Paired t-tests were used to compare spinopelvic and SI joint parameters between WBCT and NWBCT conditions. Independent t-tests were used to compare quantitative SI joint changes according to vacuum sign alteration status. Pearson correlation coefficients were used to evaluate the relationships between changes in pelvic incidence (ΔPI) and changes in SI angle, S1 subsidence, JSW, sacral slope, and S1FCA. All measurements were independently performed by two board-certified orthopedic spine surgeons using the proposed three-dimensional framework. Each observer measured each parameter twice, and the mean of the two measurements was used as the observer-level value. Interobserver agreement between the observer-level mean measurements was assessed using a two-way random-effects, absolute-agreement, single-rater intraclass correlation coefficient (ICC (2, 1)), with 95% CIs (16). Reliability was evaluated separately for measurements obtained in each position. The standard error of measurement for absolute agreement (SEM agreement) was calculated from the relevant variance components, and the minimal detectable change at the 95% confidence level (MDC_{95}) was calculated as $1.96 \times \sqrt{2} \times \mathrm{SEM} \div \sqrt{\mathrm{n}}$ for interpretation of the cohort mean. Bland–Altman analysis was additionally performed for the scores (17). Mean interobserver bias was calculated as Observer 1 minus Observer 2, and the 95% limits of agreement were calculated as the mean bias ± 1.96 standard deviations of the interobserver differences. Two-tailed p-value < 0.05 was considered statistically significant.

Results

Demographic Characteristics

Fifty older adult patients with degenerative lumbar disorders were included in the study. The mean age was 76.84 ± 6.24 years, and the cohort consisted predominantly of female patients (45 females and 5 males). Degenerative disc disease was present in 38 patients, spinal stenosis in 24, degenerative spondylolisthesis in 17, degenerative scoliosis in 16, and compression fracture in 17. Ventral SI joint vacuum phenomena were frequently observed on NWBCT, whereas dorsal vacuum signs were not observed under either WBCT or NWBCT conditions (Table 1).

Table 1
Demographic characteristics

Variable	Mean ± SD or number
Sex	
Male	5
Female	45
Age (years)	76.84 ± 6.24
Degenerative conditions (diseases)	
Spinal stenosis	24
Degenerative spondylolisthesis	17
Degenerative disc disease	38
Degenerative scoliosis	16
Compression fracture	17
Spine fusion surgery	3
Hip surgery	3
Sacroiliac joint vacuum sign	
Ventral in NWBCT (right/left)	48/49
Dorsal in NWBCT (right/left)	0/0
Ventral in WBCT (right/left)	16/21
Dorsal in WBCT (right/left)	0/0
Data are expressed as number of patients (%), mean±standard deviation	

Interobserver Reliability Assessment

All positional measurements obtained on NWBCT and WBCT demonstrated excellent interobserver reliability, with ICC (2, 1) values ranging from 0.930 to 0.987. For the WBCT–NWBCT change scores, interobserver reliability was excellent for PT and right JSW, good for SS, left JSW, and SI angle, moderate for S1 subsidence. The individual-level MDC_{95} values ranged from 3.77° to 7.25° for the angular change measures and from 0.92 to 3.50 mm for the linear change measures. The corresponding cohort-level MDC_{95} values ranged from 0.53° to 1.03° and from 0.13 to 0.49 mm, respectively. For ΔPI, the cohort-level MDC_{95} value was 1.02° lower than the observed mean ΔPI of 2.69°. Bland–Altman analysis demonstrated mean interobserver biases of − 0.38° for ΔPI (95% limits of agreement [LoA], − 7.62° to 6.87°), − 0.04° for ΔPT (LoA, − 3.81° to 3.74°), − 0.20° for ΔSS (LoA, − 7.45° to 7.05°), 0.20 mm for right ΔJSW (LoA, − 0.65 to 1.04 mm), 0.26 mm for left ΔJSW (LoA, − 0.52 to 1.04 mm), and − 0.92 mm for

ΔS1 subsidence (LoA, − 3.95 to 2.10 mm). The wider limits of agreement observed for ΔPI and ΔSS were consistent with their larger individual-level MDC_{95} values (Table 2, Fig. 5).

Table 2
Interobserver reliability of positional measurements and minimal detectable change using a three-dimensional CT-based measurement framework

Parameter	WBCT ICC (2, 1)	NWBCT ICC (2, 1)	Individual MDC_{95}	Cohort-level MDC_{95}
PI (˚)	0.954 (0.921–0.974)	0.954 (0.920–0.974)	7.25	1.02
PT (˚)	0.987 (0.974–0.993)	0.941 (0.892–0.967)	3.77	0.53
SS (˚)	0.961 (0.931–0.978)	0.947 (0.908–0.970)	7.25	1.03
Right JSW (mm)	0.930 (0.874–0.961)	0.982 (0.966–0.990)	0.92	0.13
Left JSW (mm)	0.948 (0.910–0.971)	0.965 (0.886–0.985)	0.93	0.13
SI angle (˚)	0.980 (0.963–0.989)	0.964 (0.861–0.986)	6.24	0.88
S1 subsidence (mm)	0.987 (0.977–0.993)	0.986 (0.971–0.992)	3.50	0.49

Values are presented as intraclass correlation coefficients with 95% confidence intervals, except for the minimal detectable change. Interobserver reliability was assessed using a two-way random-effects, absolute-agreement, single-rater model (ICC(2, 1)). The value recorded by each observer represented the mean of two repeated measurements. The individual-level minimal detectable change at the 95% confidence level (MDC_{95}) was calculated as 1.96 × √2 × SEM agreement, and the Cohort-level MDC_{95} was calculated as the individual-level MDC_{95} divided by √n (n = 50).
Abbreviations: WBCT, weight-bearing computed tomography; NWBCT, non–weight-bearing computed tomography; ICC, intraclass correlation coefficient; MDC, minimal detectable change; SEM, standard error of measurement; PI, pelvic incidence; PT, pelvic tilt; SS, sacral slope; JSW, joint space width; SI, sacroiliac.

Comparison of Spinopelvic Parameters Between WBCT and NWBCT Conditions

Spinopelvic parameters differed significantly between WBCT and NWBCT conditions. The mean PI was significantly greater under weight-bearing than non–weight-bearing conditions (52.04 ± 10.14° vs. 49.35 ± 9.90°, $p < 0.001$). Absolute change of PI was 2.69 ± 3.75° and the group-level relative change (mean differences divided by mean NWBCT) was 5.44%. PT also increased significantly under weight-bearing conditions (27.48 ± 10.29° vs. 11.53 ± 6.08°, $p < 0.001$), whereas SS decreased significantly (24.75 ± 11.87° vs. 37.89 ± 9.79°, $p < 0.001$). (Table 3).

Table 3
Functional changes in spinopelvic parameters and associated biomechanical factors under weight-bearing conditions

Variables	Weight-bearing	Non-weight-bearing	Statistic	p
Spinopelvic parameter changes			Δ	
PI (CT, ˚)	52.04 ± 10.14	49.35 ± 9.90	+ 2.69	< 0.001
PT (CT, ˚)	27.48 ± 10.29	11.53 ± 6.08	+ 15.95	< 0.001
SS (CT, ˚)	24.75 ± 11.87	37.89 ± 9.79	−13.14	< 0.001
Vacuum sign change analysis	Vacuum change (+) (n = 38)	Vacuum change (-) (n = 12)		
ΔSS	−14.67 ± 7.91	−9.55 ± 4.81		0.040
ΔS1FCA	0.21 ± 1.58	−0.48 ± 1.26		0.133

Data are presented as mean ± standard deviation unless otherwise specified. PI, PT, and SS were calculated using the CT-based 3D framework. Abbreviations: PI, pelvic incidence; PT, pelvic tilt; SS, sacral slope; S1FCA, S1-femur coronal angle.

Quantitative Changes in SI Joint Morphology Under Weight-Bearing Conditions

Quantitative SI joint analysis revealed significant morphological alterations under physiological loading. The SI angle decreased significantly from 36.09 ± 10.04° on NWBCT to 32.37 ± 9.33° on WBCT (Δ = −3.72 ± 5.14°, $p < 0.0001$), and S1 subsidence increased significantly under weight-bearing conditions (Δ = +3.05 ± 1.99 mm, $p < 0.0001$). In addition, bilateral JSW narrowed significantly in the standing posture (all $p < 0.001$), indicating compressive deformation of the SI articulation under physiological loading **(**Table 4**)**.

Table 4
Weight-bearing induced changes in sacroiliac joint morphology (paired-t test)

Parameter	WBCT	NWBCT	Δ	p
S1 subsidence (mm)	33.70 ± 8.52	30.65 ± 8.66	+ 3.05 ± 1.99	< 0.0001
SI angle (˚)	32.37 ± 9.33	36.09 ± 10.04	-3.72 ± 5.14	< 0.0001
Right JSW (mm)	2.01 ± 0.85	3.34 ± 1.54	-1.33 ± 1.11	< 0.001
Left JSW (mm)	1.89 ± 0.91	3.11 ± 1.30	-1.22 ± 0.86	< 0.001

Data are expressed as number, millimeter (mm) and degree (˚), mean±standard deviation. Abbreviations: SI, sacroiliac joint angle; JSW, joint space width

In subgroup analysis by ventral SI vacuum sign alteration, patients in whom the vacuum cleft disappeared under weight-bearing conditions showed significantly greater left-sided JSW narrowing than those without disappearance of the cleft (ΔJSW_left: −1.44 ± 0.75 mm vs. −0.78 ± 0.91 mm, p = 0.0085). No significant difference was observed in the right SI joint space (p = 0.4001) (Table 5).

Table 5
Effect on vacuum sign alteration on sacroiliac joint space narrowing (independent t-test)

Parameters	Vacuum change (-)	Vacuum change (+)	p
ΔJSW_Right (mm)	-1.12 ± 1.46	-1.42 ± 0.93	0.4001
ΔJSW_Left (mm)	-0.78 ± 0.91	-1.44 ± 0.75	0.0085

Data are expressed as number millimeter (mm), mean±standard deviation. Abbreviation: JSW, joint space width

Correlation Between Functional PI Change and SI Joint Deformation

Correlation analyses demonstrated that SI joint space narrowing was significantly associated with loading-related PI alteration. Greater right-sided JSW narrowing was correlated with larger ΔPI values (r = − 0.433, p = 0.0017), and left-sided JSW narrowing also showed a significant association with ΔPI (r = − 0.335, p = 0.0173). Similar associations were observed using radiographic ΔPI measurements.

In contrast, neither ΔSI angle nor ΔS1 subsidence demonstrated significant linear correlation with ΔPI (all p > 0.05). ΔSS showed no significant correlation with ΔSI angle, ΔS1 subsidence, or ΔJSW. However, ΔS1FCA demonstrated marginal correlations with bilateral ΔJSW changes (right: r = − 0.240, p = 0.0931; left: r = − 0.260, p = 0.0678).

Taken together, these findings suggest that asymmetric compressive narrowing of the SI joint may represent an important 3D biomechanical contributor to PI changes under physiological loading conditions (Table 6).

Table 6
Correlation analysis between functional spinopelvic changes and sacroiliac joint deformation parameters

Spinopelvic parameters	SI parameters	Pearson r	p
ΔS1FCA (XR)	ΔS1 subsidence (mm)	0.109	0.4522
	ΔSI angle (˚)	-0.063	0.6651
	ΔRight JSW (mm)	-0.240	0.0931
	ΔLeft JSW (mm)	-0.260	0.0678
ΔSS (CT)	ΔS1 subsidence (mm)	0.111	0.4414
	ΔSI angle (˚)	0.231	0.1072
	ΔRight JSW (mm)	-0.048	0.7392
	ΔLeft JSW (mm)	0.067	0.6438
ΔPI (CT)	ΔS1 subsidence (mm)	0.184	0.2001
	ΔSI angle (˚)	-0.127	0.3788
	ΔRight JSW (mm)	**-0.433**	**0.0017**
	ΔLeft JSW (mm)	**-0.335**	**0.0173**
ΔPI (XR)	ΔS1 subsidence (mm)	0.085	0.5577
	ΔSI angle (˚)	0.022	0.8795
	ΔRight JSW (mm)	**-0.336**	**0.0171**
	ΔLeft JSW (mm)	**-0.352**	**0.0122**

Data are expressed as the correlation coefficient wth p-value. Abbreviations: ΔPI; difference of PI between weight bearing CT and non-weight bearing CT, ΔS1-femur CA; difference of sacral to femur center angle in weight bearing x-ray and non-weight bearing x-ray, ΔSS; difference of sacral slope; SI angle, sacroiliac joint angle; JSW, joint space width.

Discussion

This study investigated the biomechanical mechanisms underlying functional PI alteration under physiological loading using a WBCT-based 3D analysis framework. The principal findings were as follows: (1) spinopelvic parameters changed significantly between WBCT and NWBCT conditions; (2) dynamic SI joint deformation, reflected by JSW narrowing, decreased SI angle, and increased sacral subsidence, occurred under loading conditions; (3) bilateral JSW narrowing was significantly correlated with loading-related PI change; and (4) ΔSS and ΔS1FCA independently contributed to weight-bearing states. These findings indicate that functional PI alteration may represent a 3D biomechanical

phenomenon associated with SI joint micromotion rather than a simple projectional or positional artifact.

Development of the WBCT-Based 3D Framework and Prior Findings

We developed a 3D CT-based spinopelvic analysis framework that reconstructs pelvic anatomical structures from DICOM datasets and automatically calculates spinopelvic parameters within a true 3D coordinate system.(13) Using this framework, we demonstrated discordance between PI measurements obtained from conventional 2D radiographs and those derived from 3D CT, suggesting that imaging modality may introduce intrinsic measurement bias even under identical weight-bearing conditions. In a subsequent comparison of WBCT and NWBCT datasets analyzed with the same 3D framework, we identified loading-dependent discordance in spinopelvic parameters. Based on these observations, we proposed two potential biomechanical contributors to functional PI variability: coronal asymmetry and SI joint instability. To characterize coronal pelvic behavior, we introduced S1FCA, while dynamic alterations in SI joint vacuum phenomena were considered potential markers of SI joint instability under loading conditions. Although the previous study demonstrated that ΔS1FCA was associated with PI change, vacuum sign alteration itself was not clearly associated with ΔPI. The present study therefore extends that work by quantitatively assessing actual SI joint micromotion during WBCT.

Quantitative Evaluation of SI Joint Micromotion

To directly evaluate SI joint micromotion under physiological loading, this study introduced quantitative SI joint parameters, including JSW, SI angle, and S1 subsidence. JSW quantified compressive narrowing between the sacral and iliac articular surfaces, whereas SI angle captured converging motion of the iliac wings under loading conditions. In addition, S1 subsidence was introduced to evaluate subtle inferior migration of the sacrum relative to the iliac ring, particularly in the ventral SI joint region. The 3D CT framework enabled flexible reconstruction of identical anatomical reference planes in standing and supine CT datasets, allowing measurements on corresponding planes despite differences in posture. S1 subsidence was standardized on identical S1 endplate-parallel planes, whereas SI angle and JSW were evaluated consistently on planes parallel to the S1 foramina. This approach supported reproducible quantitative assessment of subtle SI joint deformation and micromotion under physiological loading conditions.

SI Joint Compression as a Mechanism of Functional PI Change

A major finding of the present study was that bilateral JSW narrowing was significantly associated with PI change, whereas more generalized loading-related measures, including SI angle and S1 subsidence, were not. This distinction may be biomechanically relevant. Reductions in SI angle and increases in S1 subsidence likely reflect generalized pelvic ring deformation during standing. In contrast, JSW narrowing directly reflects compressive approximation of the sacral and iliac articular surfaces. Therefore, the

relationship between ΔJSW and ΔPI suggests that asymmetric articular compression and SI joint micromotion contribute more directly to loading-related PI variability than axial loading alone. These findings may also explain why vacuum sign alteration did not correlate directly with ΔPI in our previous study. Vacuum phenomena likely represent indirect markers of degenerative instability rather than quantitative measures of articular deformation.(18, 19) By directly assessing SI joint micromotion, the present study demonstrated that compressive narrowing of the SI articulation may represent the anatomical substrate underlying functional PI variability.

Relationship Between Sagittal Compensation, Coronal Asymmetry, and Functional PI Change

This study additionally demonstrated that ΔSS and ΔS1FCA independently contributed to functional PI change in multivariate regression analysis. These findings suggest that PI variability is not explained solely by sagittal pelvic retroversion, but rather reflects integrated 3D pelvic deformation involving sagittal and coronal compensatory mechanisms. The significant association between ΔSS and ΔPI is consistent with conventional concepts of sagittal spinopelvic compensation in degenerative spinal disorders.(2, 6) However, ΔS1FCA remained an independent contributor to loading-related PI alteration, indicating that coronal asymmetry may represent an additional biomechanical component influencing pelvic orientation during weight-bearing. Interestingly, ΔS1FCA demonstrated only marginal correlations with quantitative SI compression parameters such as ΔJSW. This finding may indicate that coronal asymmetry reflects a more heterogeneous rotational or compensatory behavior that cannot be fully explained by direct compressive narrowing alone. Accordingly, PI change may represent the combined result of SI joint compression, sagittal pelvic compensation, and asymmetric 3D pelvic rotation.

Clinical Implications

These findings have important implications for spinopelvic assessment in older adult patients with degenerative spinal disorders. Conventional spinopelvic analysis generally assumes that PI is a fixed anatomical constant.(7) However, the present findings suggest that PI may vary functionally in association with dynamic SI joint behavior under physiological loading. Therefore, reliance on static supine imaging alone may underestimate the biomechanical characteristics of the pelvis during standing. WBCT-based 3D analysis may provide additional insight into dynamic pelvic behavior and SI joint instability that cannot be fully appreciated with conventional imaging modalities.

Limitations

This study had some limitations. First, the sample size was relatively small and consisted predominantly of female older adult patients with degenerative spinal disorders, which may limit the generalizability to younger or asymptomatic populations. Second, although the present study demonstrated significant associations between SI joint deformation and functional PI alterations, causality could not be definitively established because of the observational study design. Third, the SI joint micromotion was inferred indirectly using imaging-based quantitative parameters rather than direct in vivo kinematic measurements. Fourth, although the positional PI measurements demonstrated excellent interobserver

reliability, the reliability of ΔPI was comparatively low (ICC (2, 1) = 0.489), with an individual-level MDC_{95} of 7.25°. Therefore, small changes in PI should be interpreted cautiously at the individual-patient level. However, the observed mean ΔPI exceeded the group-level MDC_{95} of 1.02°, supporting the interpretation of the loading-related PI change at the cohort level. Finally, the moderate coefficients of determination observed in the regression analyses suggested that additional biomechanical factors contributing to functional PI change remain unidentified.

Conclusion

Functional alteration of pelvic incidence under physiological weight-bearing was associated with WBCT-detected deformation of the sacroiliac joint. Bilateral SI joint-space narrowing correlated with ΔPI, suggesting that load-dependent PI variability may reflect three-dimensional deformation and subtle micromotion across the SI joint. ΔSS and ΔS1FCA were independently associated with ΔPI, further supporting a coupled response of the sacropelvic complex to loading. These findings challenge the conventional view of PI as a completely fixed anatomical parameter and suggest that it may exhibit functional variability according to loading conditions. However, because SI joint micromotion was inferred from positional differences between weight-bearing and non-weight-bearing images rather than measured directly, and because of the observational design and modest explained variance, causal or mechanistic interpretations should be made cautiously.

Declarations

Ethics Approval and consent to participate:

This study was approved by the Institutional Review Board of Korea University Anam Hospital (IRB No. 2024AN0427) and was conducted in accordance with the principles of the Declaration of Helsinki. Written informed consent to participate was obtained from all participants prior to enrollment.

Consent for publication

Not applicable.

Competing interests

The authors declare that they have no competing interests.

Funding

No external funding was received for this study.

Author Contribution

S. Lim: Data curation, Formal analysis, Writing – original draft. H.R. Lee & H.J. Kim: Data curation, Investigation. M.S Kang & T.H. Kim: Methodology, Validation. S.W. Suh & S.H. Lee: Conceptualization, Resources, Supervision. J.H. Yang: Conceptualization, Project administration, Writing – review & editing, Supervision. D.-G. Chang: Conceptualization, Methodology, Writing – review & editing. All authors read and approved the final manuscript.

Acknowledgement

This works was supported by Korea University Guro Hospital (KOREA RESEARCH-DRIVEN HOSPITAL) and grant internal funded by Korea University College of Medicine (No.O2617151). We would like to thank Editage (www.editage.co.kr) for English language editing.

Data availability

The datasets generated and/or analyzed during the current study are not publicly available due to institutional data protection regulations but are available from the corresponding author on reasonable request and with permission of the Institutional Review Board.

References

1. Vrtovec T, Pernus F, Likar B. A review of methods for quantitative evaluation of spinal curvature. Eur Spine J. 2009;18(5):593–607.
2. Barrey C, Roussouly P, Perrin G, Le Huec JC. Sagittal balance disorders in severe degenerative spine. Can we identify the compensatory mechanisms? Eur Spine J. 2011;20(5):626–33.
3. Cho Y, Jo DJ, Hyun SJ, Park JH, Yang NR. From the Spinopelvic Parameters to Global Alignment and Proportion Scores in Adult Spinal Deformity. Neurospine. 2023;20(2):467–77.
4. Le Huec JC, Thompson W, Mohsinaly Y, Barrey C, Faundez A. Sagittal balance of the spine. Eur Spine J. 2019;28(9):1889–905.
5. Celestre PC, Dimar JR 2nd, Glassman SD. Spinopelvic Parameters: Lumbar Lordosis, Pelvic Incidence, Pelvic Tilt, and Sacral Slope: What Does a Spine Surgeon Need to Know to Plan a Lumbar Deformity Correction? Neurosurg Clin N Am. 2018;29(3):323–9.
6. Le Huec JC, Aunoble S, Philippe L, Nicolas P. Pelvic parameters: origin and significance. Eur Spine J. 2011;20(5):564–71.
7. Legaye J, Duval-Beaupere G, Hecquet J, Marty C. Pelvic incidence: a fundamental pelvic parameter for three-dimensional regulation of spinal sagittal curves. Eur Spine J. 1998;7(2):99–103.
8. Lee KY, Lee JH, Im SK, Lee WY. Analysis of measurement changes in pelvic incidence according to pelvic rotation using a three-dimensional model. BMC Musculoskelet Disord. 2022;23(1):110.

9. Fujita N, Yagi M, Watanabe K, Nakamura M, Matsumoto M, Yokoyama Y, et al. Determining the validity and reliability of spinopelvic parameters through comparing standing whole spinal radiographs and upright computed tomography images. BMC Musculoskelet Disord. 2021;22(1):899.
10. Moon JW, Shinn JK, Ryu D, Oh SY, Shim YS, Yoon SH. Pelvic Incidence Can Be Changed not only by Age and Sex, but also by Posture Used during Imaging. Korean J Spine. 2017;14(3):77–83.
11. Zhu W, Wang Y, Kong C, Sun X, Pan F, Wang W, et al. A Comprehensive Analysis of the Behavior of Pelvic Incidence After Different Posterior Spinal Procedures in Elderly Patients With Spinal Deformity. Global Spine J. 2023;13(2):368–77.
12. Nagamoto Y, Iwasaki M, Sakaura H, Sugiura T, Fujimori T, Matsuo Y, et al. Sacroiliac joint motion in patients with degenerative lumbar spine disorders. J Neurosurg Spine. 2015;23(2):209–16.
13. Lim S, Kim HJ, Lee SH, Kim TH, Kang MS, Suh SW, et al. Discordance in spinopelvic alignment between weight-bearing and supine positions on three-dimensional computed tomography. J Clin Neurosci. 2026;151:112063.
14. Boulay C, Tardieu C, Hecquet J, Benaim C, Mouilleseaux B, Marty C, et al. Sagittal alignment of spine and pelvis regulated by pelvic incidence: standard values and prediction of lordosis. Eur Spine J. 2006;15(4):415–22.
15. Vleeming A, Schuenke MD, Masi AT, Carreiro JE, Danneels L, Willard FH. The sacroiliac joint: an overview of its anatomy, function and potential clinical implications. J Anat. 2012;221(6):537–67.
16. Koo TK, Li MY. A Guideline of Selecting and Reporting Intraclass Correlation Coefficients for Reliability Research. J Chiropr Med. 2016;15(2):155–63.
17. Bland JM, Altman DG. Statistical methods for assessing agreement between two methods of clinical measurement. Lancet. 1986;1(8476):307–10.
18. Takata Y, Higashino K, Morimoto M, Sakai T, Yamashita K, Abe M, et al. Vacuum Phenomenon of the Sacroiliac Joint: Correlation with Sacropelvic Morphology. Asian Spine J. 2016;10(4):762–6.
19. Asada M, Tokunaga D, Arai Y, Oda R, Fujiwara H, Yamada K, et al. Degeneration of the Sacroiliac Joint in Hip Osteoarthritis Patients: A Three-Dimensional Image Analysis. J Belg Soc Radiol. 2019;103(1):36.

Figures

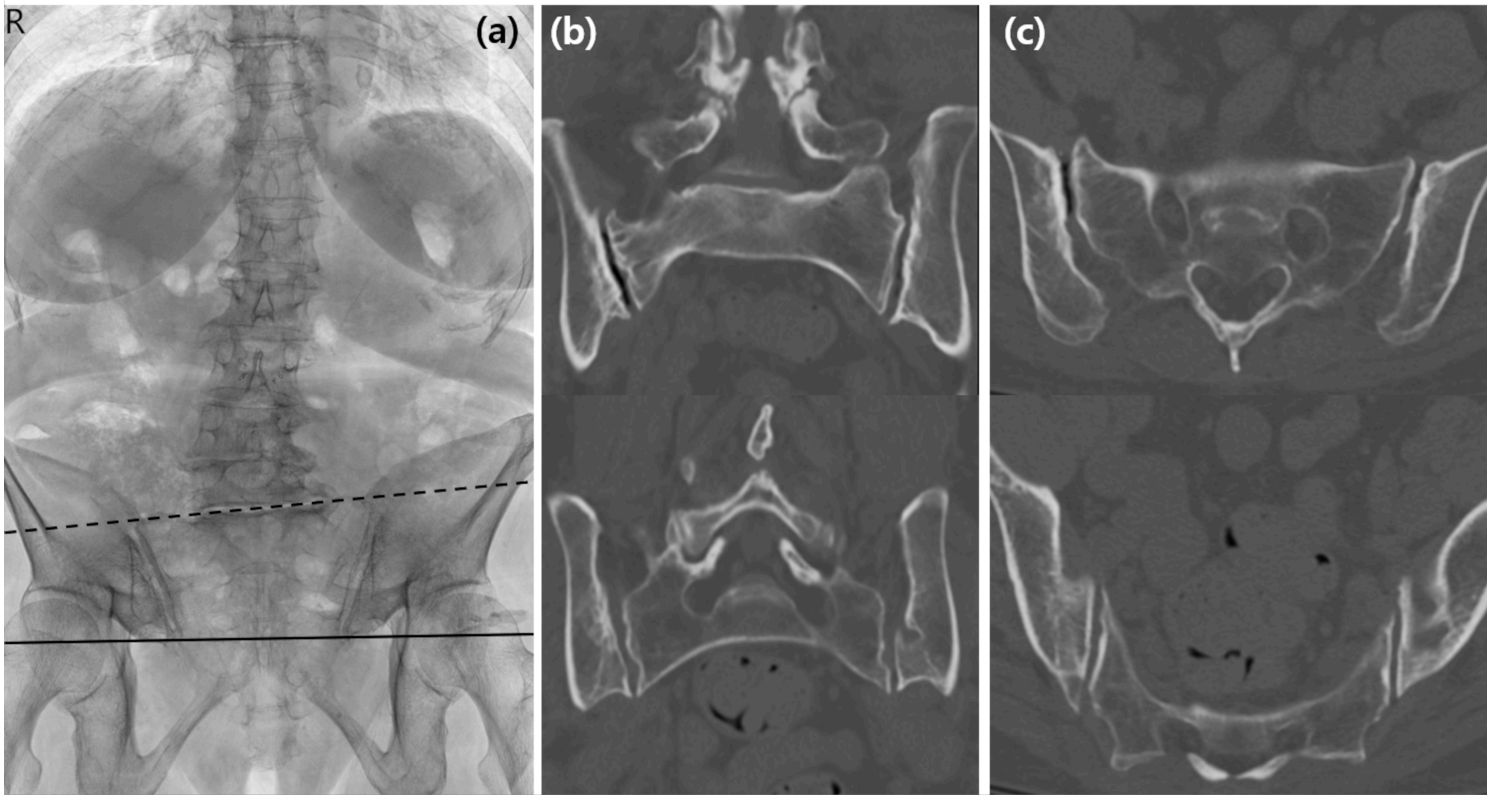


Figure 1

X-ray image demonstrating the S1-femur coronal angle (S1FCA) (a). The black dotted line represents the extended line of the sacral endplate or sacral alae, while the black solid line represents the line connecting the centers of both femoral heads. The angle formed between these two lines was defined as the S1-femur coronal angle (S1FCA). CT images demonstrating vacuum signs in the ventral cartilaginous portion and dorsal ligamentous portion of the sacroiliac joint (b, coronal view; c, axial view).

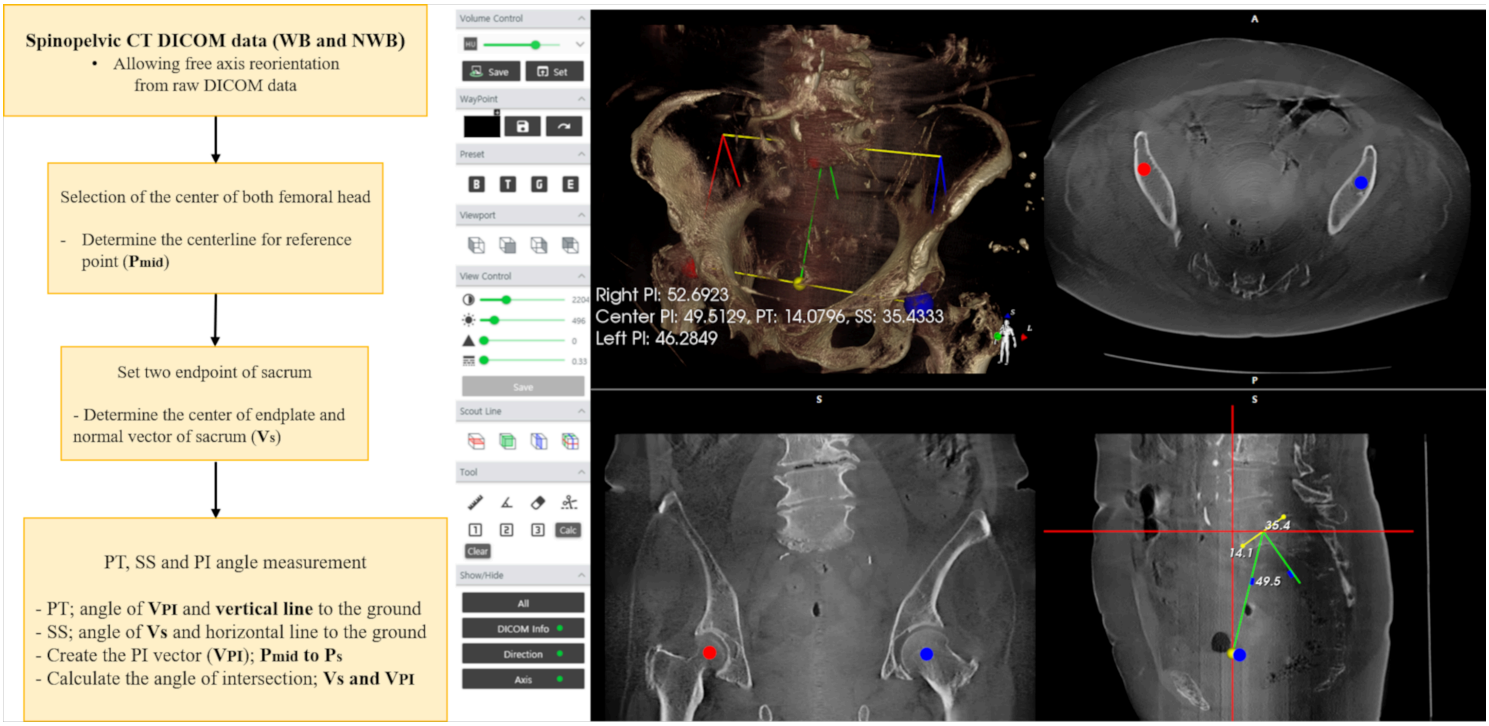


Figure 2

A schematic diagram of the overall structure of the pelvic alignment analysis algorithm and the final implemented framework. After defining the centers of the left and right femoral heads and the anterior and posterior margins of the sacral endplate, the program automatically calculates sacral slope, pelvic tilt, and pelvic incidence.

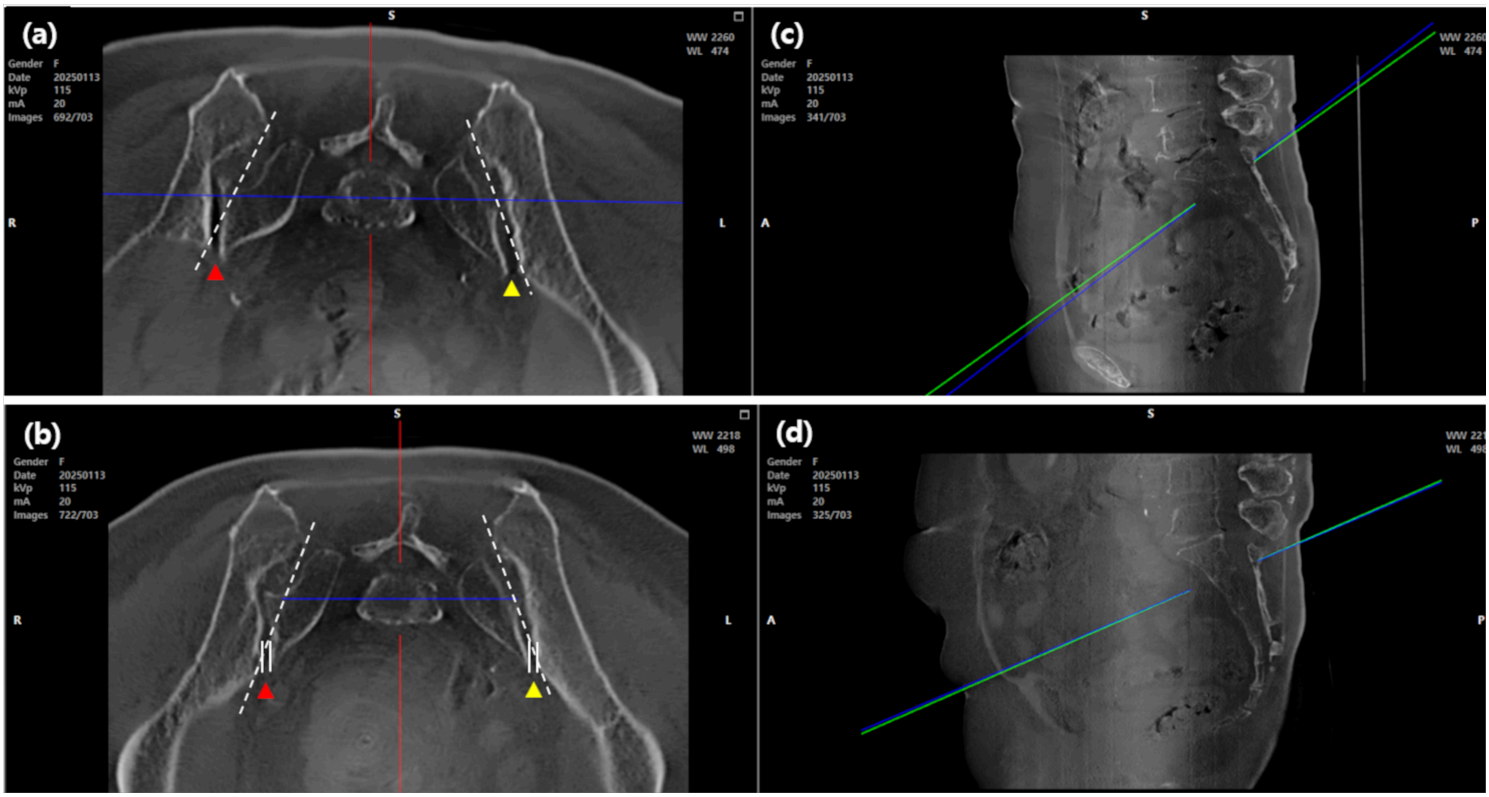


Figure 3

Measurements of sacroiliac joint space width (SI JSW) and sacroiliac angle (SI angle) on weight-bearing CT (WBCT) and non–weight-bearing CT (NWBCT) using the CT-based three-dimensional framework (a, b, respectively). The red arrows indicate the right SI joint space width, while the yellow arrows indicate the left SI joint space width. The white dotted lines represent the two reference lines forming the SI angle. Prior to measurement of JSW and SI angle, the reference plane was reoriented parallel to the S1 foramina to ensure that measurements in both WBCT and NWBCT were obtained on identical anatomical planes, thereby improving measurement reproducibility (c, d, respectively).

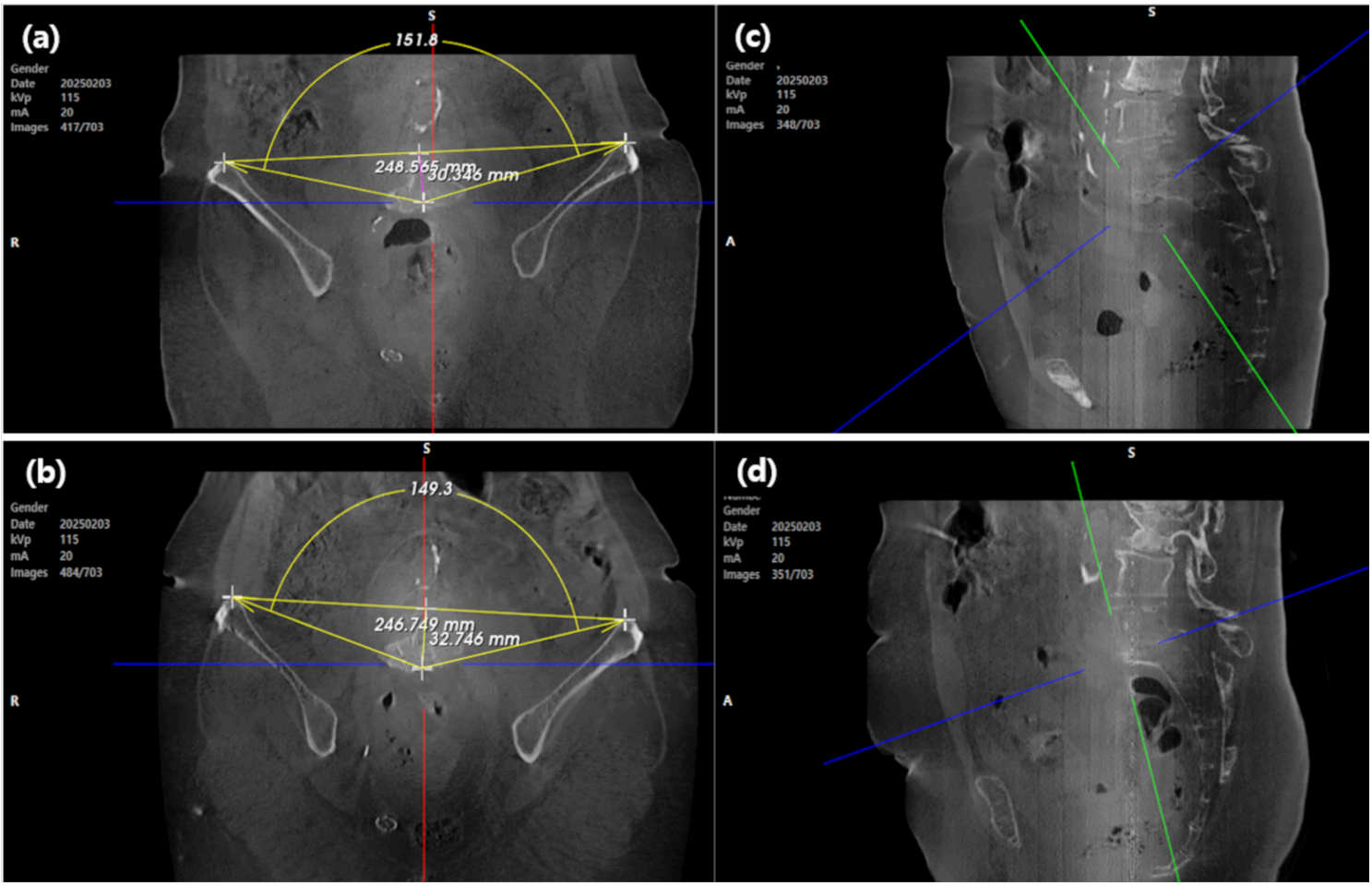


Figure 4

Measurements of sacroiliac joint subsidence (S1 subsidence) on weight-bearing CT (WBCT) and non–weight-bearing CT (NWBCT) using the CT-based three-dimensional framework (a, b, respectively). Similar to the measurements of sacroiliac joint space width and sacroiliac angle, the measurement tool within the framework was used to calculate the perpendicular distance from the anterior sacral surface tip to the line connecting both iliac crests. Prior to measurement, the plane of the sacral endplate and the plane perpendicular to it were designated as reference planes to ensure that measurements in both WBCT and NWBCT were obtained on identical anatomical planes, thereby improving measurement reproducibility (c, d, respectively).

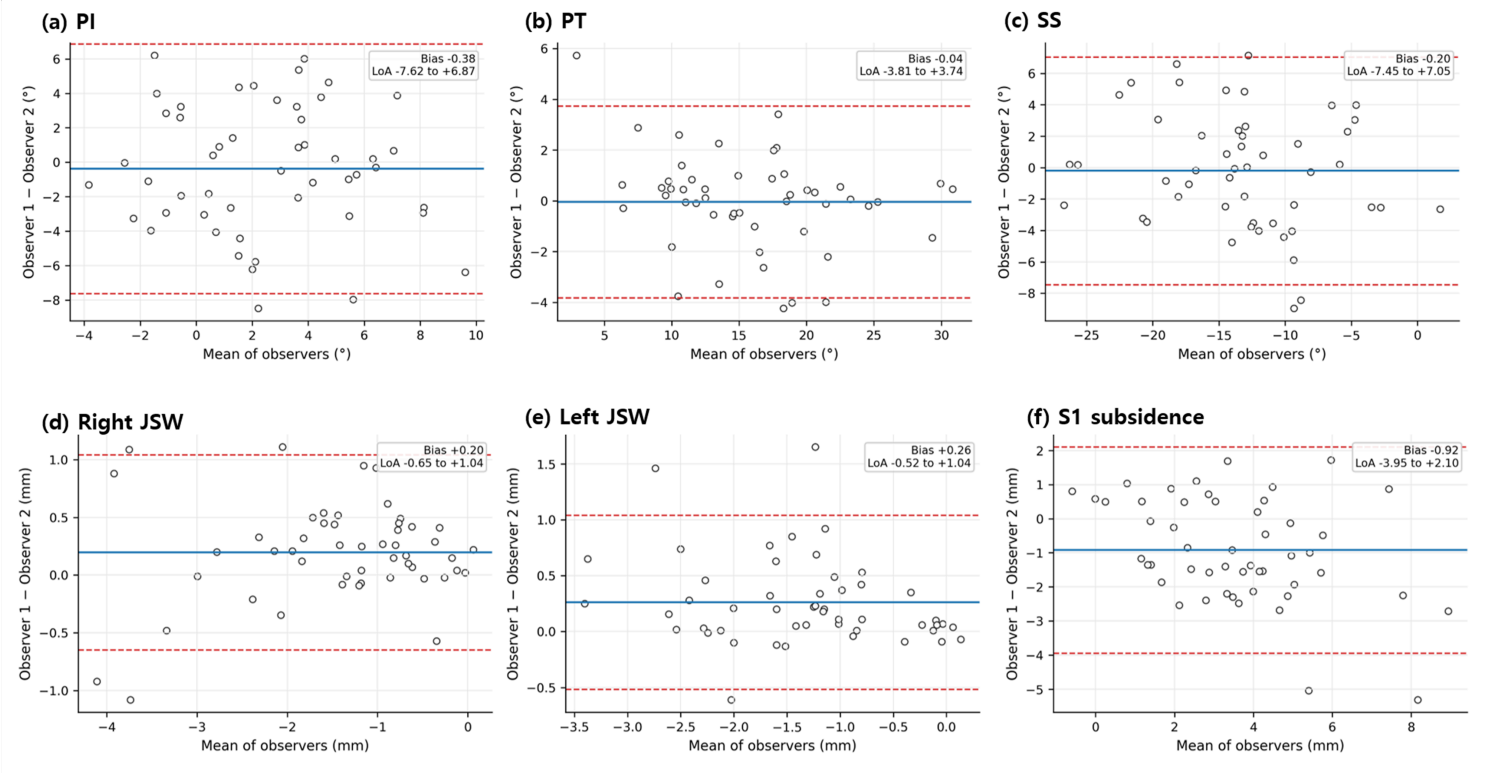


Figure 5

Bland–Altman analysis of interobserver agreement for WBCT–NWBCT change scores. Bland–Altman plots demonstrating interobserver agreement for WBCT–NWBCT change scores in (a) pelvic incidence, (b) pelvic tilt, (c) sacral slope, (d) right sacroiliac joint space width, (e) left sacroiliac joint space width, and (f) S1 subsidence. The horizontal axis represents the mean of the change scores obtained by the two observers, and the vertical axis represents the difference between observers (Observer 1 minus Observer 2). The solid blue line indicates the mean interobserver bias, and the dashed red lines indicate the 95% limits of agreement. Each observer-level value was derived from the mean of two repeated measurements. Change scores were calculated as WBCT minus NWBCT.